ISSN 0915-6364

NATIONAL INSTITUTE FOR FUSION SCIENCE

One-electron Capture and Target Ionization in He^+-neutral-atom Collisions.

V.P. Shevelko, D. Kato, M-.Y. Song, H. Tawara,
I.Yu. Tolstikhina and J-.S. Yoon

(Received - July 28, 2009)

NIFS-DATA-107 Dec. 11, 2009

RESEARCH REPORT
NIFS-DATA Series

TOKI, JAPAN

One-electron capture and target ionization in He^+-neutral-atom collisions.

V.P. Shevelko[1*], D. Kato[2], M-.Y. Song[3], H. Tawara[2, 4], I.Yu.Tolstikhina[1] and J-.S. Yoon[3]

[1] P.N. Lebedev Physical Institute, Leninskii pr. 53, Moscow 119991, Russia

[2] National Institute for Fusion Science, Toki, Japan

[3] National Fusion Research Institute, Gwahangno 113, Yuseong-Gu, Daejeon, Korea

[4] Max Planck Institute for Nuclear Physics, Saupfercheckweg 1, 691171 Heidelberg, Germany

Abstract.

One-electron capture and target-ionization cross sections in collisions of He^+ ions with neutral atoms:

$He^+ + A \rightarrow He + A^+$ and $He^+ + A \rightarrow He^+ + A^+ + e$, A = H, He($1s^2$, 1s2s), Ne, Ar, Kr, Xe,

are calculated and compared with available experimental data over the broad energy range E = 0.1 keV/u – 10 MeV/u of He^+ ions. The role of the metastable states of neutral helium atoms in such collisions, which are of importance in plasma physics applications, is briefly discussed. The recommended cross section data for these processes are presented in a closed analytical form (nine-order polynomials) which can be used for a plasma modeling and diagnostics.

Key words: one-electron capture, target ionization, metastable helium atoms, recommended cross sections

---

***)** Corresponding author. Tel.: +7-499-7833684; fax: +7-499-1352408. *E-mail address*:

v.chevelko@gsi.de

(V. Shevelko).

1. Introduction.

Charge-changing cross sections of atomic collisions involving H and He particles and their ions with neutral atoms are needed in many applications related with controlled thermonuclear fusion research (plasma heating by injection of neutral-particle beams, plasma diagnostics using a probe-beam attenuation), industrial plasmas, astrophysics, physics of upper atmosphere and others. Experimental data and theoretical calculations of electron capture and ionization cross sections are presented in many books and review articles (see, e.g., [1 - 13]). It has already been shown that the first-order perturbation theory can be applied for cross-section calculations at relatively high impact energies, especially, for collisions of bare ions (protons, H^+, α-particles). At low collision energies, molecular-orbital theories are usually applied [11] but the accurate predictions can be made only when the problem can be reduced to a three-body problem, i.e., one electron in the field of two Coulomb centers. The most complicated for consideration are collisions involving dressed projectiles at intermediate energy when electrons of both colliding particles participate in the process (see, e.g., [14 - 16]).

In the present work, extensive numerical calculations are performed for the following charge-changing processes involving He^+ projectiles colliding with neutral atoms, namely, of one-electron capture into the projectile ions

$$He^+ + A \rightarrow He + A^+, \quad (1)$$

and one-electron ionization of target atoms

$$He^+ + A \rightarrow He^+ + A^+ + e, \quad (2)$$

for A = H, He (including He^*(1s2s)), Ne, Ar, Kr, and Xe atomic targets, using various models and computer codes valid for low and high impact energies. Combining theoretical results with available experimental data, a set of the recommended data are presented in a closed analytical form over a wide range of He^+ energy E = 0.1 keV/u – 10 MeV/u using a nine-order polynomial fitting. In the case of He^+ + He collisions, the influence of the metastable 1s2s states of He atoms on the charge-changing and ionization cross sections is briefly discussed.

In the following, the atomic units $m_e = e = \hbar = 1$ are used where m_e and e denote the electron mass and charge, respectively, and $\hbar$ the Planck constant.

2. Recommended cross sections and analytical fittings.

In the present work, electron capture and ionization cross sections for reactions (1) and (2) were calculated using available computer codes (ARSENY, CAPTURE, LOSS. CDW) described in Appendix. The contribution from all target electrons is taken into account. Calculated cross sections are presented in section 3 and compared with experimental data and other calculations in a wide collision energy range.

In all figures, the recommended cross sections σ_{rec} are also displayed. They are obtained by choosing the reliable experimental and theoretical data, or, if no experimental data are available, by using the following formula [17]:

$$\frac{1}{\sigma_{rec}} = \frac{1}{\sigma_{low}} + \frac{1}{\sigma_{high}}, \tag{3}$$

where σ_{low} and σ_{high} denote the cross sections calculated at low (ARSENY code) and high (CAPTURE and CDW codes) energies, respectively. This formula matches the cross sections at medium energy range using well-defined cross sections at low and high energies.

All recommended cross sections are found to be well fitted by the nine-order polynomials within 20 % accuracy in the form:

$$\log_{10}\left(\sigma_{rec}[cm^2]\right) = \sum_{i=0}^{9} A_i \left(\log_{10} E[keV/u]\right)^i . \tag{4}$$

The fitting parameters A_i for one-electron capture and ionization processes are given in Tables 1 - 3. The energy range where eq. (4) can be applied is given in the last column of the tables.

3. Numerical calculations and comparison with experiment.

In this section, experimental and theoretical one-electron capture and target-ionization cross sections in collisions of He^+ ions with neutral atoms are given. Calculations include mainly the data obtained by using several computer codes: ARSENY code for capture and ionization at low energies, CDW and CAPTURE codes for electron capture at high energies, and LOSS code for ionization at high energies. A brief description of the codes and theoretical methods used are given in Appendix.

3.1 Capture cross sections.

a) $He^+ + H$ collisions.

Capture cross sections for this reaction are shown in Fig. 1. At energies E > 100 keV/u, all results obtained in the Born approximation are very close to each other. As a recommended cross section, we adopted the experimental data from [13] in the whole energy range. The fitiing parameters, eq. (4), are given in Table 1.

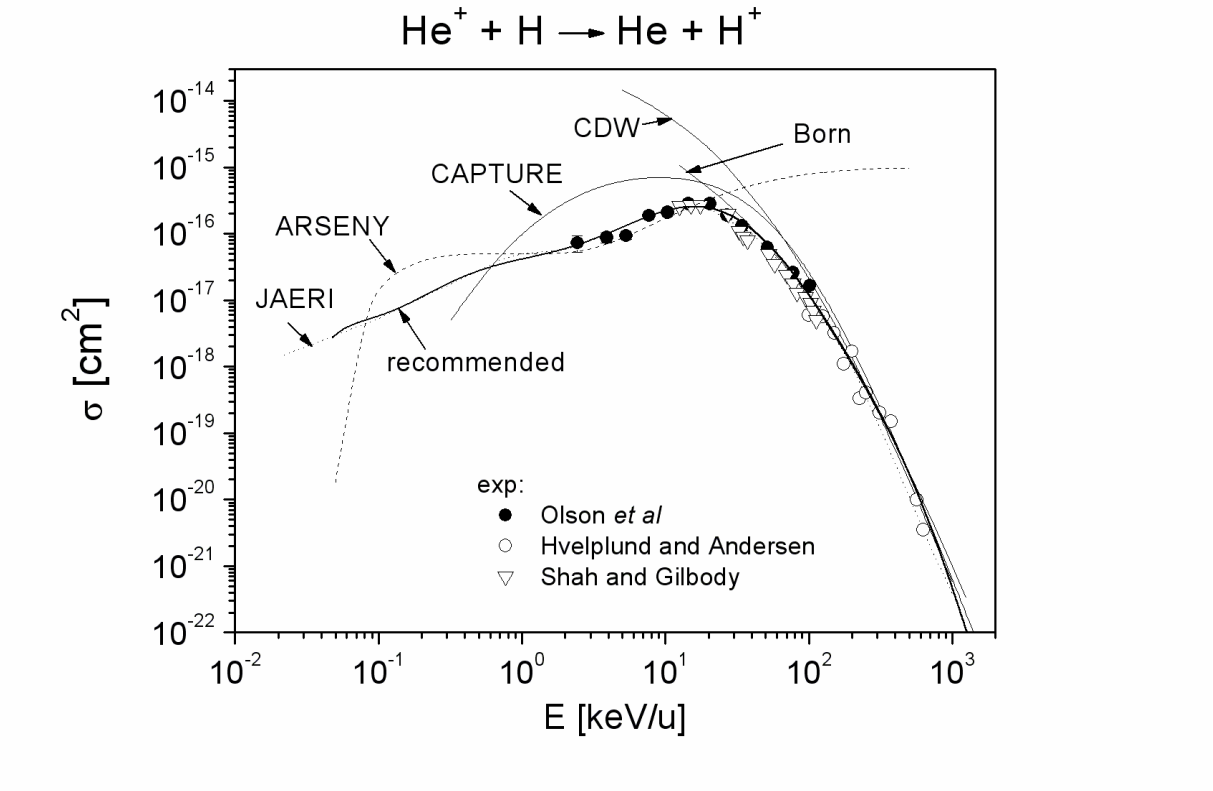

Fig. 1. Total electron-capture cross sections in $He^+ + H$ collisions as a function of He^+ energy. Experiment: ● [18], ○ [19], ∇ [20]. Dotted line – recommended cross section from [13] based on the experimental data. Theory: Born – Born approximation [21], ARSENY – ARSENY code, CAPTURE – CAPTURE code, CDW – CDW code, present work. Thick solid curve - recommended cross section from [13] which is described by eq. (4) with fitting parameters given in Table 1.

b) He^+ + He collisions.

i) He target in the ground state: $He^+(1s) + He(1s^2) \rightarrow He + He^+(1s)$.

Figure 2 shows the total one-electron capture cross sections, covering seven orders of He^+ energy, in collisions with the ground state helium atom, $He(1s^2)$. Experimental data are taken from compilations [10] and [13] and other sources shown in the figure. In this reaction, the main contribution at low energies comes from the resonance electron capture (see Fig. 5). In the whole energy range considered (7 orders of magnitude), the best results are presented by the CAPTURE code and coincide with the recommended data [13] except for those in a narrow range around ~ 50 keV/u. The ARSENY code fails at low energies because it is unable to describe correctly the resonance electron capture processes. The electron capture cross sections in the Born approximation [21] at E > 800 keV/u are higher than the recommended data in [13] which we adopted as the recommended capture cross section.

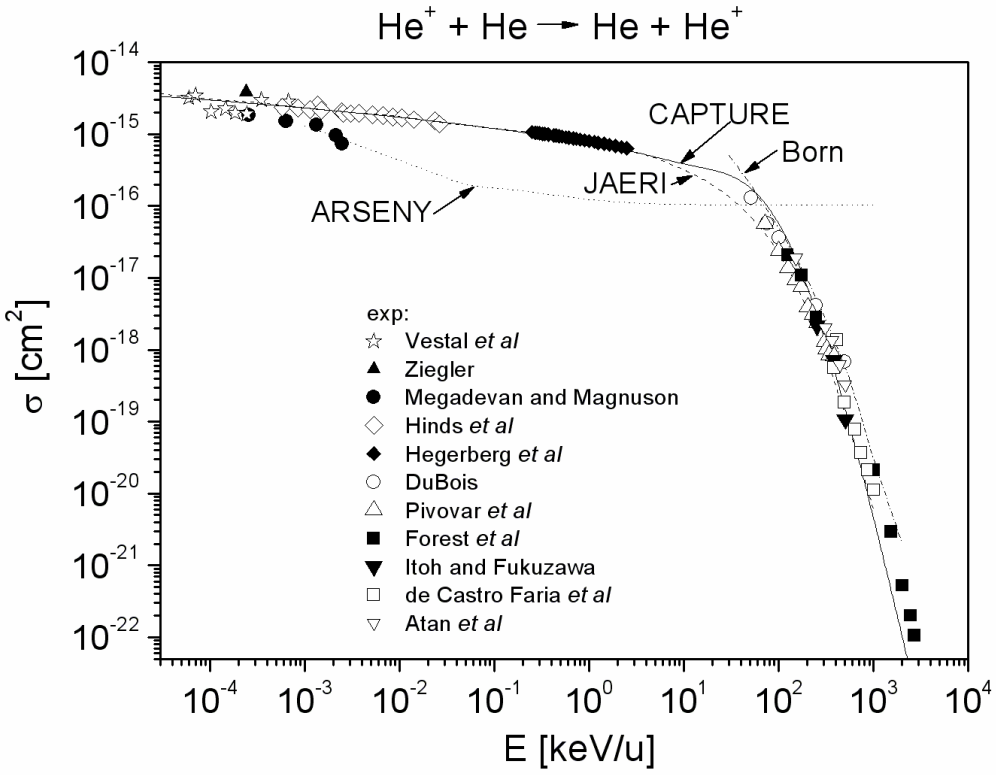

Fig. 2. Total electron-capture cross sections in collisions of He^+ ions with the ground-state He atoms as a function of He^+ energy. Experiment: ☆[22], ▲[23], ●[24], ◇[25], ◆[26], ○[27], △[28], ■[29], ▼[30], □[31], ▽[32], Dashed line – recommended cross section from [13].
Theory: Born – Born approximation [21], ARSENY – ARSENY code, CAPTURE – CAPTURE code. As the recommended cross section, we adopt the data [13] which are fitted by eq. (4) with fitting parameters given in Table 1.

ii) He target in the metastable (1s2s) state: $He^+(1s) + He^*(1s2s) \rightarrow He + He^+(1s)$.

Figure 3 shows the total one-electron capture cross section in collisions of He^+ ions with excited He*(1s2s) atoms as a function of He^+ energy, i.e., summed over all states of He atom in the final channel, calculated by the CAPTURE code. Contribution from capture of 1s and 2s electrons is shown by two dashed curves. At energies E < 50 keV/u the main contribution comes from the resonance capture, i.e., capture of 2s electron of the target into 2s state of He^+ ions, resulting in He*(1s2s) excited state atom. On the other hand, capture of 1s electron becomes dominant at energy E > 100 keV/u. A small bump around E ~ 5 keV/u is due to contribution of different excited states (n > 2) of He atom in the final channel. To our knowledge, no experimental data for this reaction have been reported so far.

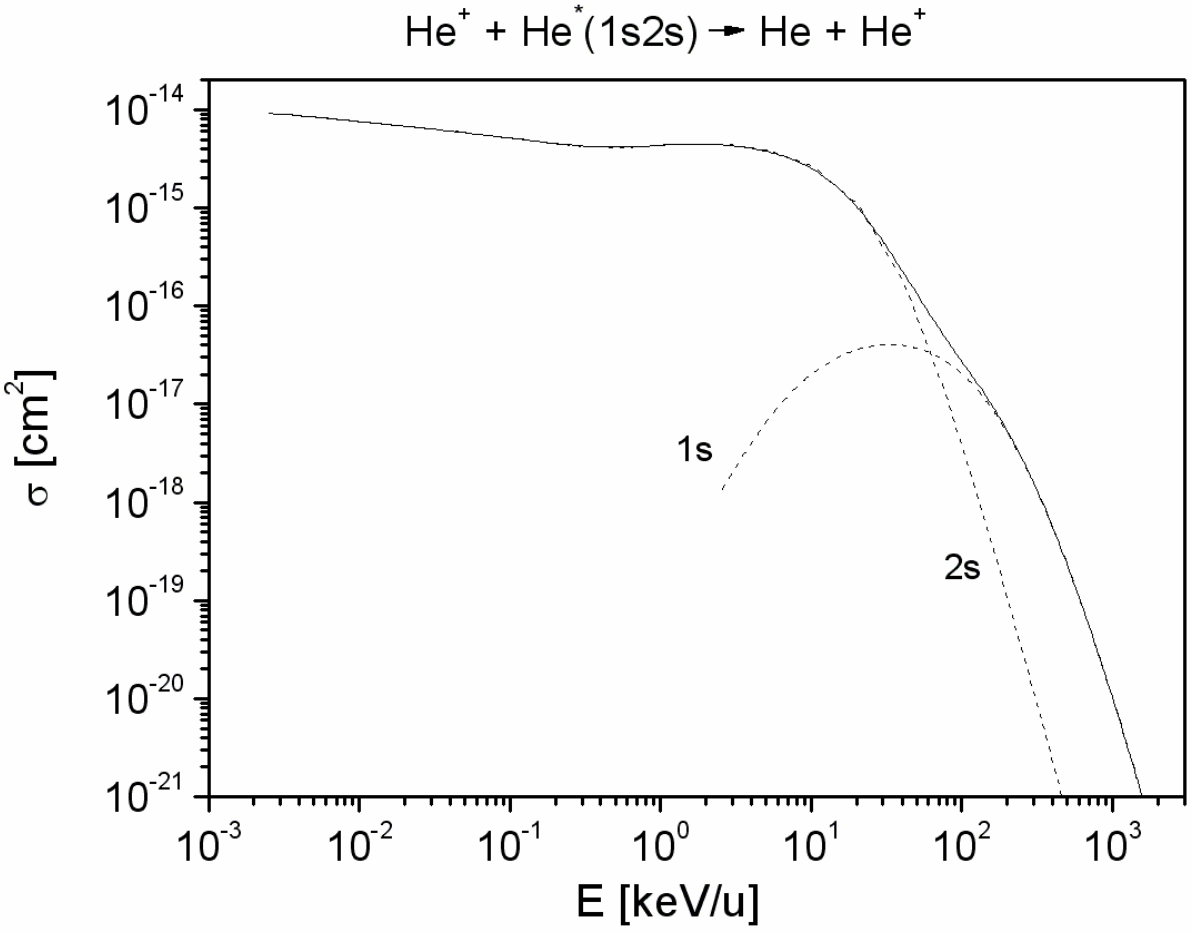

Fig. 3. Total one-electron capture cross sections in collisions of He^+ ions with excited He*(1s2s) atoms as a function of He^+ energy. Dashed curves marked with 1s and 2s – contribution from capture of 1s and 2s electrons of excited He target into all possible states of the resulting He atom. ARSENY – ARSENY code, CAPTURE – CAPTURE code; solid curve – recommended cross section, eq. (4) and Table 1.

iii) State-selective electron capture: $He^{+}(1s) + He^{*}(1s2s) \rightarrow He^{*}(1s^2) + He^{+*}(2s)$, i.e., electron transition 1s → 1s.

Calculated state-selective capture cross sections for this reaction is shown in Fig. 4. At low energies, we adopted the data calculated by ARSENY code while at high energies those by the CAPTURE code. In the intermediate energy range, the data were matched with the help of eq. (3). The recommended cross section is shown by a thick solid curve which was fitted by eq. (4) with parameters given in Table 2.

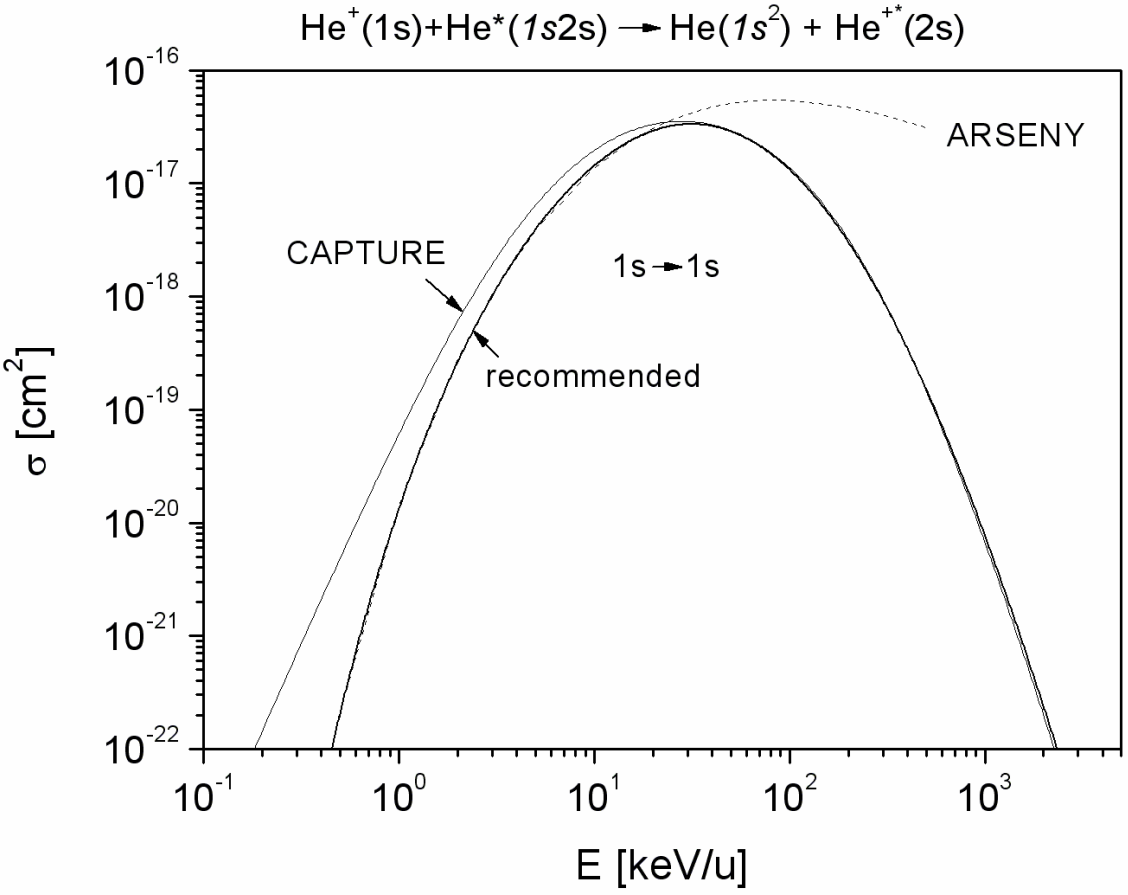

Fig. 4. Calculated state-selective capture cross sections for reaction $He^{+}(1s) + He^{*}(1s2s) \rightarrow He(1s^2) + He^{+*}(2s)$, i.e., transition 1s → 1s: dashed curve – ARSENY code, thin solid curve – CAPTURE code, thick solid curve – recommended cross section, eqs. (3), (4) and Table 2.

iv) State-selective *resonance* capture: $He^+(1s) + He^*(1s2s) \rightarrow He^*(1s2s) + He^+(1s)$, i.e., transition 2s → 2s.

Calculated state-selective capture cross section for this resonance reaction is shown in Fig. 5. Due to the resonance character, the cross section increases with energy decreasing.

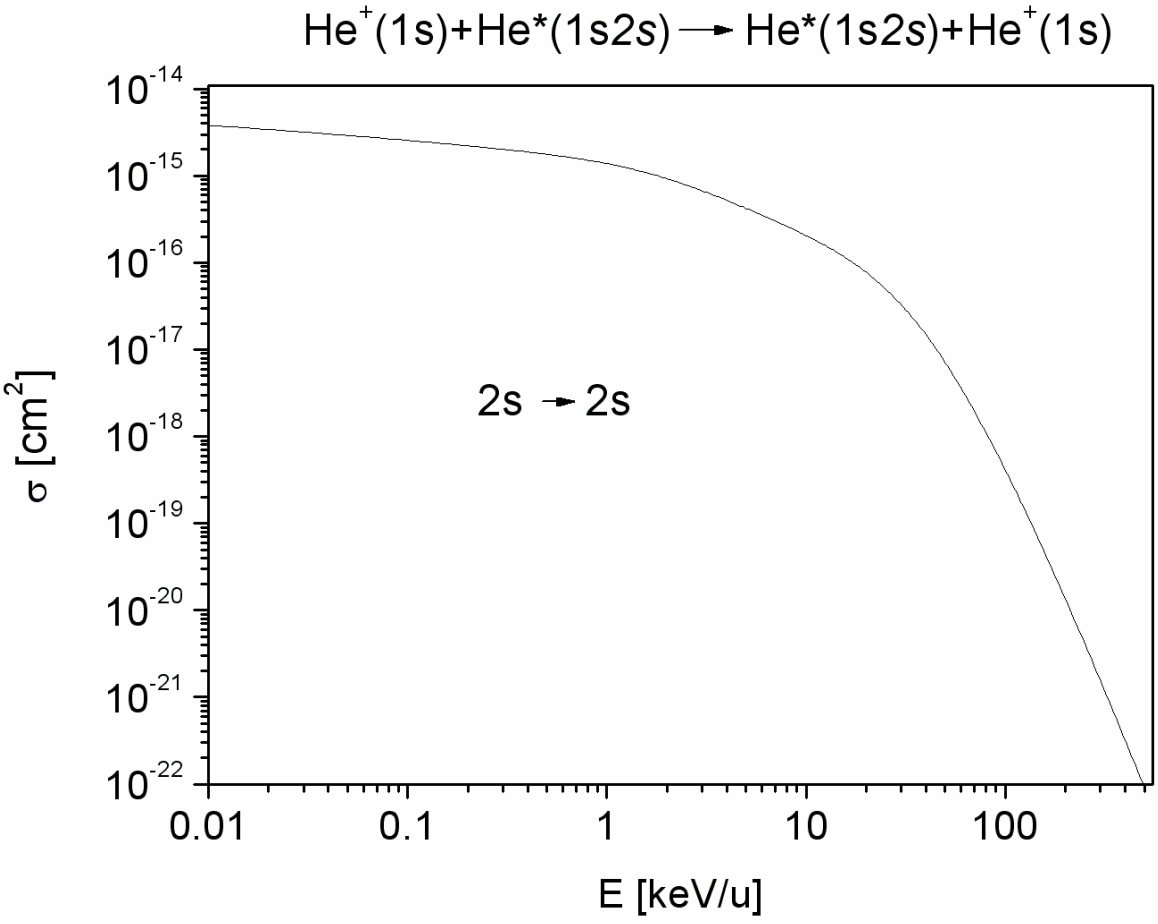

Fig. 5. Calculated state-selective capture cross sections for the *resonance* reaction $He^+(1s)+ He^*(1s2s) \rightarrow He^*(1s2s) + He^+(1s)$, i.e., transition 2s → 2s, calculated by the CAPTURE code. Recommended cross sections are presented by eq. (4) with fitting parameters given and Table 2.

c) He^+ + Ne collisions.

One-electron capture cross sections in collisions of He^+ ions with Ne atoms are displayed in Fig. 6. At high energies, we adopted the data obtained by the CDW code. The results given by the CAPTURE code largely overestimate experimental data at low energies (< 0.1 keV/u) where the reaction has a quasi-resonance character: the binding energy of the outermost $2p^6$ shell electron (21.6 eV) of Ne atom is fairly close to the binding energy of He atom in the final ground state (24.6 eV). For this reason, the ARSENY code is unable to describe correctly the capture cross section at low energy range.

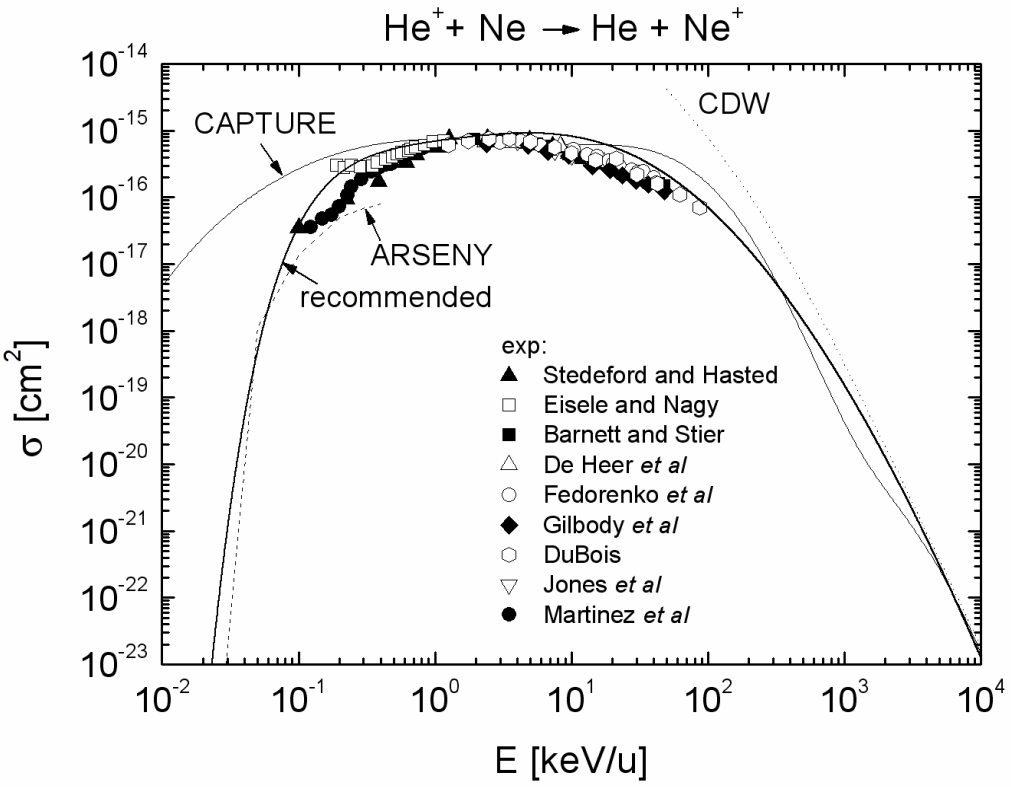

Fig. 6. **O**ne-electron capture cross sections in collisions of He^+ ions with Ne atoms as a function of He^+ energy. Experiment: ○[1], ⬡[27], ▲[33], □[34], ■[35], △[36], ◆[37], ▽[38], ●[39]. Theory: dashed curve – ARSENY code, thin solid curve - CAPTURE code, dotted curve – CDW code, thick solid curve – recommended cross section, eq. (4) and Table 1.

d) He^+ + Ar collisions.

Experimental and theoretical capture cross sections in collisions of He^+ ions with Ar atoms are given in Fig. 7. At low energies we adopted experimental values [27] as our recommended data whereas at high energies the recommended cross section is normalized to the CDW results.

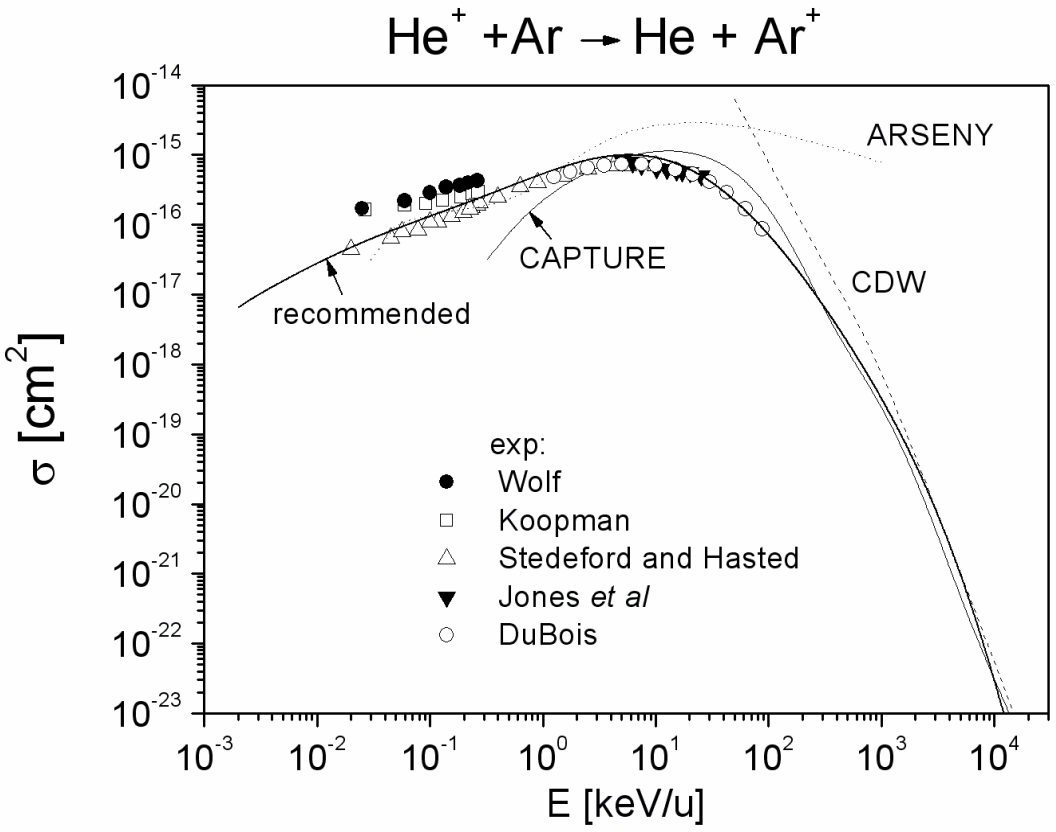

Fig. 7. **O**ne-electron capture cross sections in collisions of He^+ ions with Ar atoms as a function of He^+ energy. Experiment: ○[27], △[33], ▼[38], ●[40], □[41]. Theory: dotted curve – ARSENY code, dashed curve – CDW code, thin solid curve - CAPTURE code, thick solid curve – recommended cross section, eq. (4) and Table 1.

e) He^+ + Kr collisions.

Experimental and theoretical data for one-electron capture from Kr is shown in Fig. 8. At high energies there is quite good agreement between theory and experiment while at low energies (< 0.1 keV/u) the data of Stedeford and Hasted [33] and Koopman [41] differ significantly from each other. We chose the data [33] which are closer to our calculations by ARSENY code.

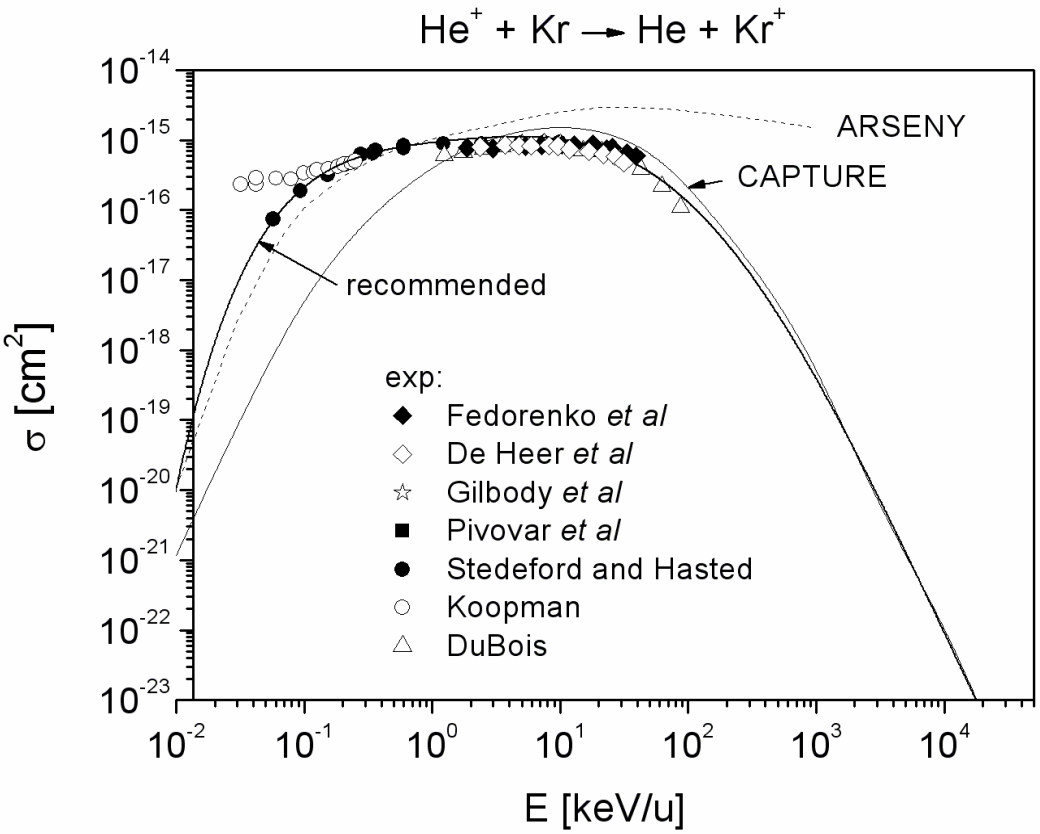

Fig. 8. Total electron-capture cross sections in collisions of He^+ ions with Kr atoms as a function of He^+ energy. Experiment: ◆[1], △[27], ■[28], ●[33], ◇[36], ○[41], ☆ [42]. Theory: dotted curve – ARSENY code, dashed curve – CDW code, thin solid curve - CAPTURE code, thick solid curve – recommended cross section, eq. (4) and Table 1.

f) He^+ + Xe collisions.

Total electron-capture cross sections in collisions of He^+ ions with Xe atoms are shown in Fig. 9. At low energy range, the reaction has a quasi-resonance character because the binding energy of the inner $5s^2$ shell in Xe, 23.4 eV, is very close to the binding energy of He atom in the final channel, 24.6 eV, and, therefore, the cross sections are rather large.

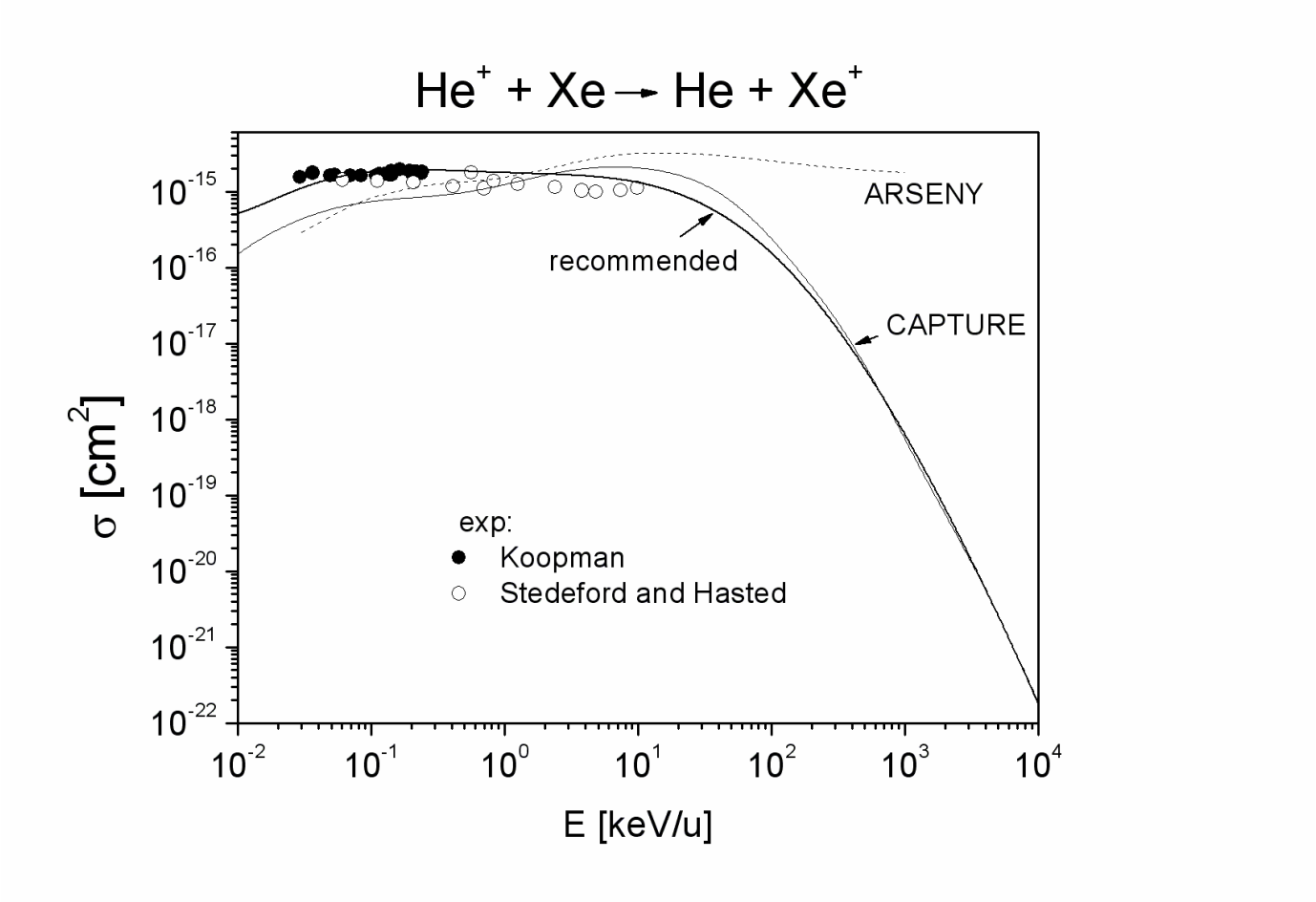

Fig. 9. Total electron-capture cross sections in collisions of He^+ ions with Xe atoms as a function of He^+ energy. Experiment: ◯[33], ●[41]. Theory: dashed curve – ARSENY code, thin solid curve - CAPTURE code, thick solid curve – recommended cross section, eq. (4) and Table 1.

3.2 Ionization cross sections.

Experimental and calculated one-electron ionization cross sections of H, He, Ne, Ar, Kr and Xe atoms by He^+ ions are shown in Figs. 10 - 15. At low and high energies they were calculated by ARSENY and LOSS code, respectively. Except for H target, the recommended cross sections were obtained by using eq. (3) and are in a good agreement with available experimental data. In case of H target, the recommended cross section was determined from calculations by ARSENY and LOSS codes and available experimental data.

Recommended ionization cross sections σ of He in the ground, $He(1s^2)$ and excited, He*(1s2s), states are shown in Figs. 11 and 12. They were obtained on the basis of calculations by ARSENY and LOSS codes (no experimental data are known). Below cross-section maximum occurring at ~ 100 keV/u, σ(1s2s) is much higher than $\sigma(1s^2)$ since their binding energies differ significantly: 4.5 and 24.6 eV, respectively. At higher energies, the calculated ratio is $\sigma(1s2s)/\sigma(1s^2) \approx 2.5$ which is in good agreement with the Born results: σ is proportional to the number of the equivalent electrons of the target shell and inversely proportional to its binding energy. It means that $\sigma(1s2s) : \sigma(1s^2) \approx 1/4.5 : 2/24.6 \approx 2.5$. The contribution from ionization of 1s electron into σ(1s2s) is very small because its binding energy in He*(1s2s) is rather large: $I(1s) \approx 54$ eV.

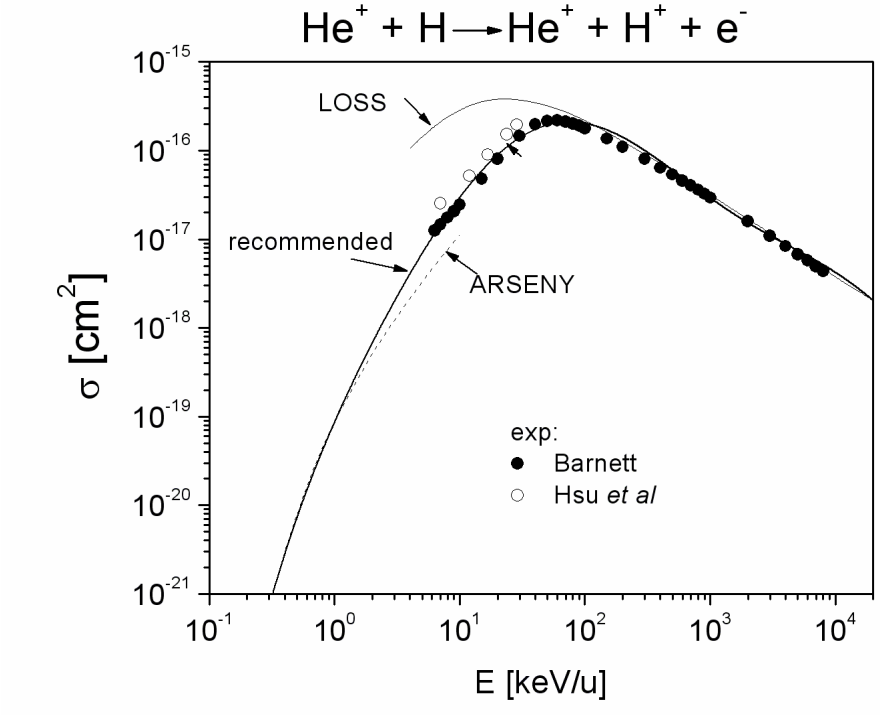

Fig. 10. Ionization cross sections of H(1s) atom by He^+ as a function of He^+ energy. Experiment: ●[10], ○[43]. Theory: dashed curve – ARSENY code, thin solid curve - LOSS code, thick solid curve – recommended cross section, eq. (4) and Table 3.

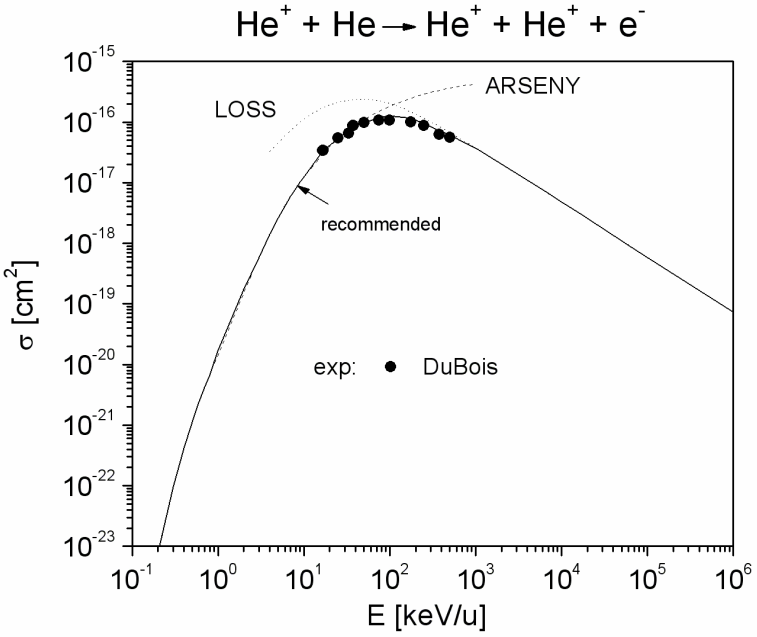

Fig. 11. One-electron ionization cross sections of $He(1s^2)$ atom by He^+ ion as a function of He^+ energy. Experiment: ●[27]. Theory: dashed curve – ARSENY code, dotted curve - LOSS code, solid curve – recommended cross section, eqs. (3), (4) and Table 3.

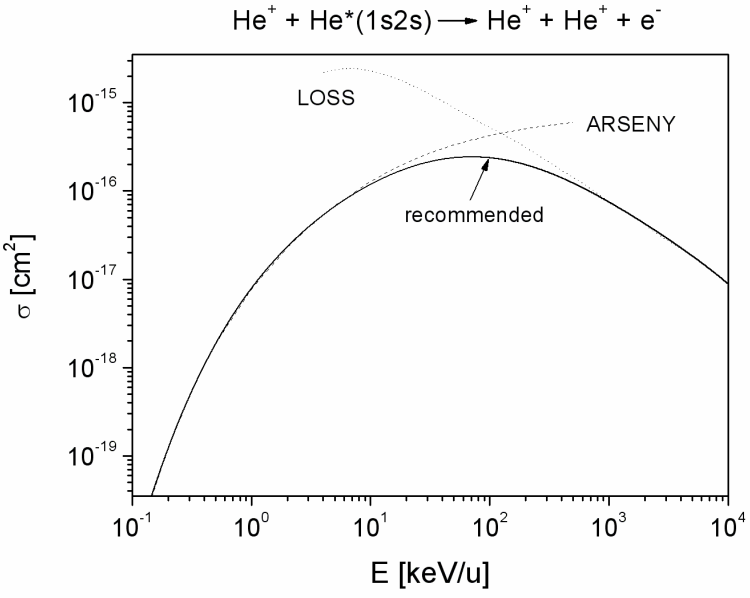

Fig. 12. Calculated one-electron ionization cross sections of excited helium atom, He*(1s2s), by He^+ ion, i.e., the sum of ionization cross sections of 1s and 2s electrons in $He^*(1s2s)$ target as a function of He^+ energy. Theory: dashed curve – ARSENY code, dotted curve - LOSS code, solid curve – recommended cross section, eqs. (3), (4) and Table 3.

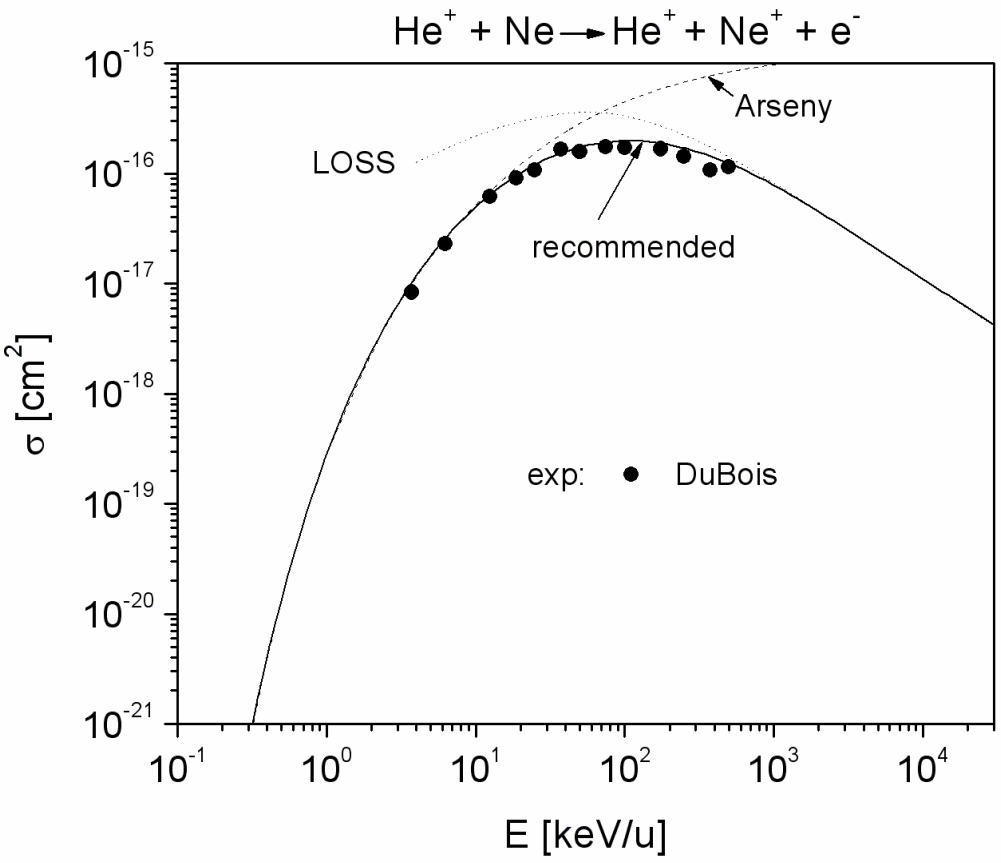

Fig. 13. One-electron ionization cross sections of Ne atoms by He^+ ions as a function of He^+ energy. Experiment: ●[27]. Theory: dashed curve – ARSENY code, dotted curve - LOSS code, solid curve – recommended cross section, eqs. (3), (4) and Table 3.

Experimental and calculated one-electron ionization cross sections of Ar atoms by He^+ are shown in Fig. 14. At low and high energies they were calculated with ARSENY and LOSS code, respectively. At intermediate-energy range, cross section matched using eq. (3) is in good agreement with experimental data [27].

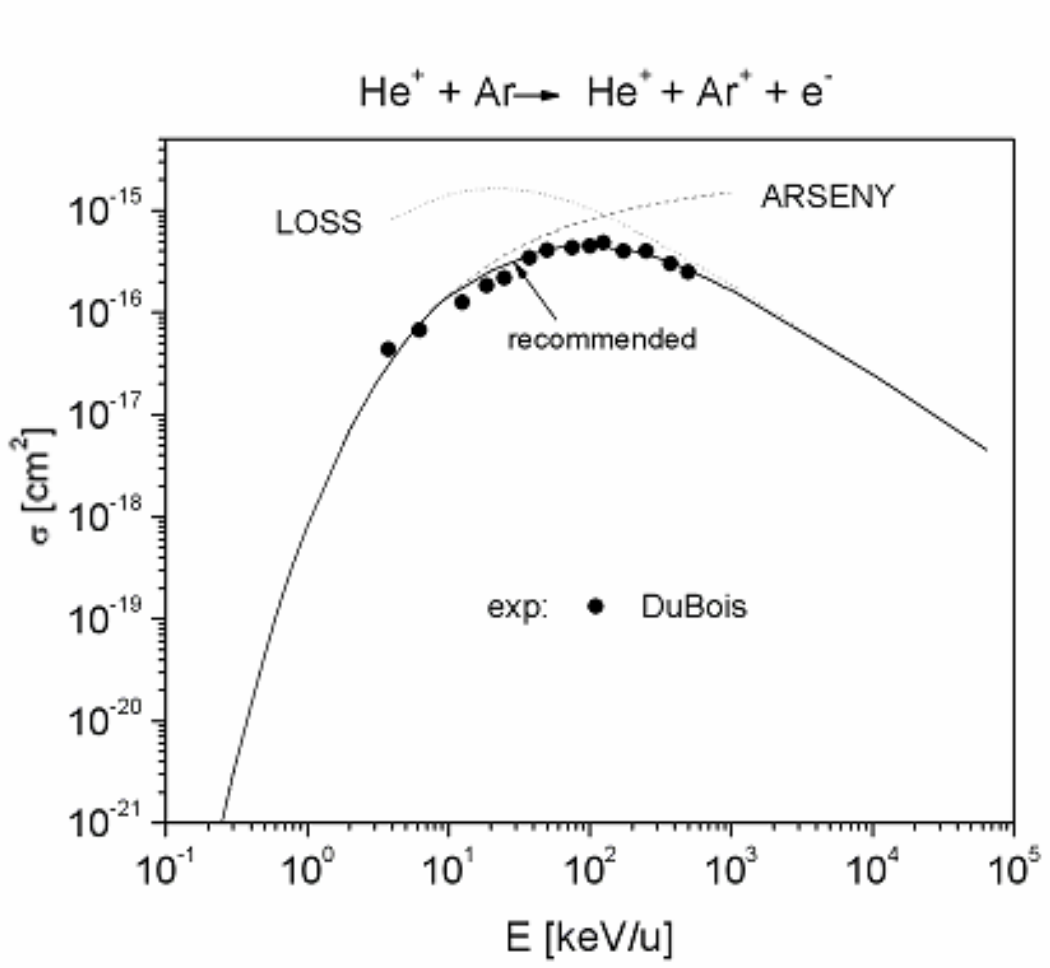

Fig. 14. One-electron ionization cross sections of Ar atoms by He^+ ions as a function of He^+ energy. Experiment: ●[27]. Theory: dashed curve – ARSENY code, dotted curve - LOSS code, solid curve – recommended cross section, eqs. (3), (4) and Table 3.

Experimental and calculated one-electron ionization cross sections of Kr atoms by He^+ are shown in Fig. 15. At low and high energies they were calculated by ARSENY and LOSS code, respectively. At intermediate energies, the cross sections were matched using eq. (3) and are in a good agreement with experimental data [26].

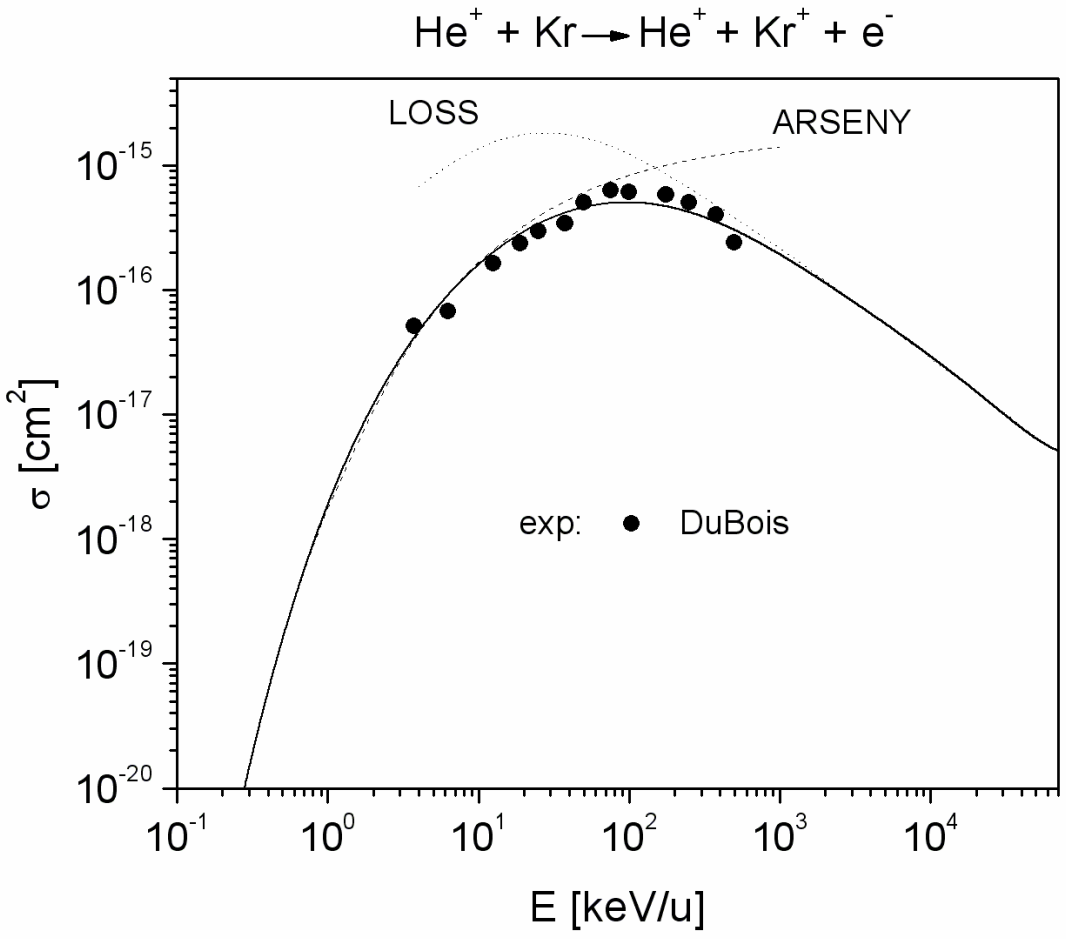

Fig. 15. One-electron ionization cross sections of Kr atoms by He^+ ions as a function of He^+ energy. Experiment: ●[27]. Theory: dashed curve – ARSENY code, dotted curve - LOSS code, solid curve – recommended cross section, eqs. (3), (4) and Table 3.

Calculated one-electron ionization cross sections of Xe atom by He^+ are shown in Fig. 16. At low and high energies they were calculated by ARSENY and LOSS code, respectively, and at intermediate energies were matched using eq. (3).

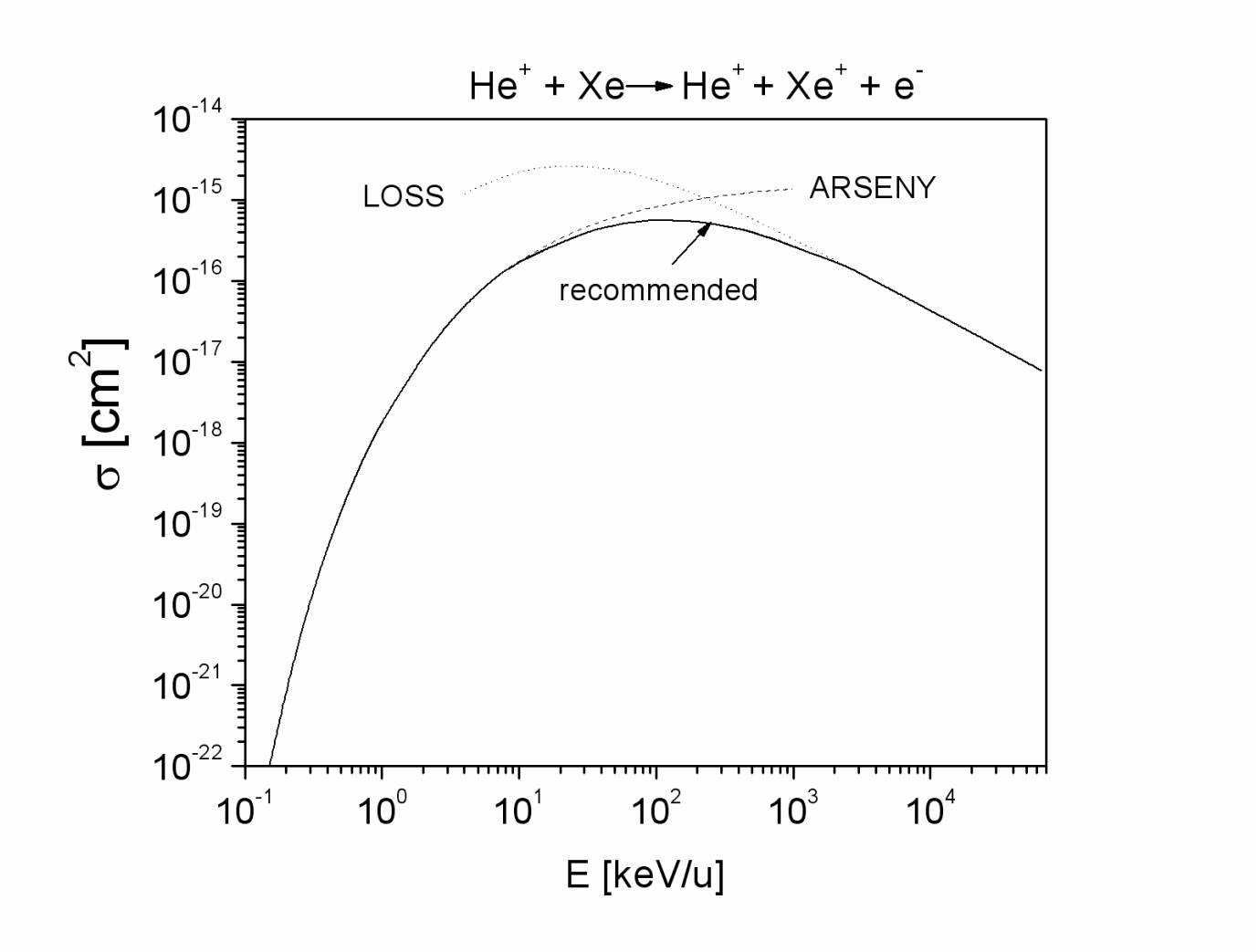

Fig. 16. One-electron ionization cross sections of Xe atoms by He^+ ions as a function of He^+ energy. Theory: dashed curve – ARSENY code, dotted curve - LOSS code, solid curve – recommended cross section, eqs. (3), (4) and Table 3.

Conclusion.

Extensive calculations of one-electron capture and target ionization cross sections in collisions of He^+ ions with H, He($1s^2$, 1s2s), Ne, Ar, Kr, Xe are performed in a wide energy range using several computer codes. Combining the calculated cross sections with available experimental data, recommended cross sections are suggested and fitted by a nine-power polynomial. The corresponding fitting parameters are given for all cases including electron capture and ionization in collisions with excited He*(1s2s) atoms. These parameters can be used for plasma modeling purposes.

Acknowledgements.

The work was performed under the RFBR grant No. 08-02-00005-a and partially under the NIFS/NINS project of Foundation Network for Scientific collaboration.

Appendix. Theoretical treatments and computer codes.

A. The ARSENY code for ionization and electron capture at low energy.

The ARSENY code is intended for calculation of one-electron capture and ionization cross sections at low energies, i.e., below the cross-section maximum [44, 45]. The code is based on the adiabatic approximation for inelastic transitions of one-electron in the two-Coulomb-centre system (Z_1, e, Z_2) where Z_1 and Z_2 are the effective charges of the target and projectile particles, respectively. These transitions occur in the regions of the closest approach of potential curves via their hidden crossings in the complex R-plane where R is the inter-nuclear separation between two nuclei.

The transition probability $P_{\alpha\beta}(b)$ between two adiabatic states α and β is given

$$P_{\alpha\beta}(b) = \exp(-2\Delta_{\alpha\beta}),\ \Delta_{\alpha\beta} = \left| \mathrm{Im} \int_{\mathrm{Re}\,R_c}^{R_c} \frac{1}{\mathrm{v}(R,b)} \left[E_\beta(R) - E_\alpha(R)\right] dR \right| , \qquad (5)$$

where b denotes the impact parameter, v the relative collision velocity of two nuclei, $E_\beta(R)$ and $E_\alpha(R)$ the energies of the final and initial states at the separation distance R, respectively, and R_c a complex branching point, or 'hidden crossing' of the two potential energy surfaces. In the adiabatic approximation, no wave functions and matrix elements are required to calculate probability $P_{\alpha\beta}(b)$. The ARSENY code gives incorrect results in the case of resonance or quasi-resonance capture reactions, i.e., when the binding energies of the captured electron before and after collision are equal or very close to each other.

B. The CDW code for electron capture at high energy.

The CDW code [46, 47] is intended for calculation of one-electron capture cross sections at high projectile energies and is based on the Continuum Distorted-Wave (CDW) approximation which is a modification of the second Born approximation. The code is able to calculate the nl capture cross sections at projectile energies given approximately by

$$E\ [\mathrm{keV}] > 50\ \max\ (I_1,\ I_2), \qquad (6)$$

where n and l are the principal and angular momentum quantum numbers, I_1 and I_2 the binding energies (in eV) of the active electron before and after collision, respectively.

In the CDW approximation, a connection between the long-range Coulomb distortion effects and the accompanying perturbation potentials is taken into account (see [46, 48]) and a single-electron approximation is used: during a collision, the *active* electron makes a transition while all other electrons are *passive* ('spectators'): their orbitals remain to be frozen. The bound states of the active electron are described by Clementi-Roetti or hydrogen-like wave functions while the intermediate continuum states by the Coulomb wave functions. In the hydrogen-like wave functions, the following effective charge $Z_{\rm eff}$ is used:

$$Z_{eff} = n(2I_{nl}^{RHF})^{1/2} \quad , \tag{7}$$

where $I^{\rm RHF}$ denotes the binding energy variationally obtained using the Roothaan-Hartree-Fock (RHF) model and Clementi-Roetti wave functions (see [46]). In general, the $Z_{\rm eff}$ value in eq. (7) is very close to the well-known estimation $Z_{\rm eff} = n(2I_{\rm nl})^{1/2}$ where $I_{\rm nl}$ is the experimental or theoretical binding energy of the *nl* state.

C. The CAPTURE code for electron capture.

The CAPTURE code is intended for calculating the probabilities P(b,v) and cross sections $\sigma_{\rm n}$(v) for one-electron capture in ion-atom and ion-ion collisions at intermediate and high energies [49]. Here b and v represent the impact parameter and the projectile velocity, respectively, and n the principal quantum number of the final state. The ℓ-components of the capture cross sections are not calculated in the CAPTURE code but estimated by the statistical distribution. The formulae, realized in the code, are based on the normalized Brinkman-Kramers (BK) approximation in the impact parameter representation. The total cross section $\sigma_{\rm tot}$ is given by the sum of partial cross sections $\sigma_{\rm n}$ for all target electron shells and all possible final states with the principal quantum number n in the projectile ion as a function of collision velocity v:

$$\sigma_{tot}(\mathrm{v}) = \sum_{n=n_0}^{n=n_{cut}} \sigma_n(\mathrm{v}), \;\; \sigma_n(\mathrm{v}) \equiv \sum_{\gamma} \sigma_{\gamma n}(\mathrm{v}), \tag{8}$$

$$\sigma_{\gamma n}(\mathrm{v}) = 2\pi \int_0^{\infty} P_{\gamma n}^{(norm)}(b,\mathrm{v})\, b\, db, \quad P_{\gamma n}^{(norm)}(b,\mathrm{v}) = \frac{P_{\gamma n}(b,\mathrm{v})}{1 + \sum_{n'=n_0}^{n_{max}} P_{\gamma n'}(b,\mathrm{v})} \tag{9}$$

where $P_{\gamma \rm n}(b,\mathrm{v})$ denotes the electron capture probability from the initial target shell γ into the final n-state of the resulting ion, including the ground state n_0, and $n_{\rm max}$ the maximum principal quantum number taken into account. The summation is made over all shells γ of the target. Here the index *norm* refers to the normalized probability and $n_{\rm cut}$ is a parameter strongly depending on the target density: for low-density gas targets it equals to infinity while in a dense target it can be small due to the so-called *target-density effects* (see [50]). In the present paper we adopt $n_{\rm cut} = \infty$ as the target density is low. The normalized capture

probability $P^{(norm)}{}_{\gamma n}(b,v)$ in eq. (9) is always less than unity, making it possible to extend the BK approximation to much lower energies than is used in the pure BK approximation.

In the CAPTURE code, the hydrogen-like wave functions $R_{nl}{}^{H}(r)$ are used for both projectile and target particles:

$$R_{nl}(r) = Z_{eff}^{3/2}\, R_{nl}^{H}(Z_{eff} r),\;\; Z_{eff} = n(2E^{RHF})^{1/2} \tag{10}$$

where Z_{eff} is already given in eq. (7). The use of hydrogen-like wave functions allows one to include excited states of the resulting ion up to very high principal quantum numbers n_{max} ~1000. This is very important in the case of highly charged projectile ions.

D. The LOSS code for ionization of the target atom.

In the present work, the LOSS code [51] is used for calculating one-electron ionization cross sections of the target atoms at relatively high energies (over the cross-section maximum) and is based on the non-relativistic Born approximation using the Schrödinger radial wave functions calculated numerically by the code.

In the LOSS code, the ionization cross section is calculated in the partial-wave representation in the momentum-transfer Q space in the form:

$$\sigma_{ion}(v) = \frac{8\pi}{v^2} \sum_{T} \sum_{\lambda} \int_0^{\infty} d\varepsilon \int_{Q_{min}}^{\infty} \frac{dQ}{Q^3} \left|F_T(Q,\varepsilon,\lambda)\right|^2 \cdot \left|F_P(Q)\right|^2, \tag{11}$$

where F_T and F_P are the target-atom form-factor and the effective charge of the incident particle, respectively, ε and λ denote the energy and orbital momentum of an ejected electron, I_T its binding energy in the target, $Q_{min} = (I_T + \varepsilon)/v$. The sum on T in eq. (11) is made over all target-shell electrons.

The target form-factor is given by

$$\left|F_T(Q,\varepsilon,\lambda)\right|^2 = \left|\left\langle \varepsilon\lambda \left| \exp(i\vec{Q}\vec{r}) \right| nl \right\rangle_T\right|^2 \tag{12}$$

where the radial wave functions of the initial (nl) and final (ελ) states are calculated numerically by solving the Schrödinger equation in the effective field of the atomic core. The effective charge of the incident heavy particle is calculated in the form:

$$\left|F_P(Q)\right|^2 = \left[Z_P - \sum_{j=1}^{N} \left\langle j \left| \exp(i\vec{Q}\vec{r}) \right| j \right\rangle \right]^2 + \left[N - \sum_{j=1}^{N} \left| \left\langle j \left| \exp(i\vec{Q}\vec{r}) \right| j \right\rangle \right|^2 \right] \tag{13}$$

with the nodeless Slater wave functions |j>. Here Z_P and N denote the nuclear charge and number of electrons in the incident particle, respectively. In the case of He^+ projectile, the function $F_P(Q)$ has a simple analytical form [51]:

$$\left|Z_{He^+}(Q)\right|^2 = \left[2 - \frac{1}{(1+Q^2/64)^2}\right]^2 + \left[1 - \frac{1}{(1+Q^2/64)^4}\right] \qquad (14)$$

References

[1] N.V. Fedorenko, V.V. Afrosimov, D.M. Kaminker, Soviet Phys.-JTP **1**, 1861 (1957).

[2] S.K. Allison, Rev. Mod. Phys. **30,** 1137 (1958).

[3] D.R. Bates (ed.), *Atomic and Molecular Processes*. (Academic Press, NY, 1962).

[4] N.V. Fedorenko, Soviet Phys.-JTP **4**0, 2481 (1970).

[5] H. Tawara, A. Russek, Rev. Mod. Phys. **45**, 178 (1973)

[6] E.E. Nikitin, S.Y. Umanskii, *Theory of Slow Atomic Collisions* (Springer, Berlin, 1984).

[7] H.B. Gilbody, Adv. Atom. Mol. Phys. **22**, 143 (1986).

[8] R.K. Janev, L.P. Presnyakov, V.P. Shevelko, *Physics of Highly Charged Ions* (Springer, Berlin, 1985).

[9] R.K. Janev, W.D. Langer, K. Evans, Jr., D.E. Post. *Elementary Processes in Hydrogen-Helium Plasmas: Cross Sections and Reaction Rate Coefficients* (Springer, Berlin, 1987).

[10] C.F. Barnett (ed.), Report ORNL-6086 (Oak Ridge National Laboratory, 1990).

[11] M. Kimura, L.F. Lane, Adv. At. Mol. Phys. **26**, 79 (1990)

[12] B.H. Bransden, M.R.C. McDowell, *Charge Exchange and the Theory of Ion-Atom Collisions*. (Clarendon, Oxford, 1992).

[13] R. Ito, T. Tabata, T. Shirai, R.A. Phaneuf, Analytic cross sections for collisions of H, H_2, He and Li atoms and ions with atoms and molecules. I. Report JAERI-M-117

(Japan, 1993); R. Ito, T. Tabata, T. Shirai, R.A. Phaneuf. Analytic cross sections for collisions of H, H_2, He and Li atoms and ions with atoms and molecules. III. Report JAERI-Data/Code 95-008 (Japan, 1995)

[14] E.C. Montenegro, W.E. Meyerhof, J.H. McGuire, Adv. At. Mol. Opt. Phys. **34**, 249 (1994)

[15] T. Kirchner, M. Horbatsch, H.J. Lüdde, J. Phys. B, **37**, 2379 (2004)

[16] I.Yu. Tolstikhina, P.R. Goncharov, T. Ozaki, S. Sudo, N. Tamura, V.Yu. Sergeev. Report NIFS-DATA-102 (NIFS, Japan, 2008)

[17] J.M. Rost, Th. Pattard, Phys. Rev. A **55**, R5 (1997)

[18] R.E. Olson, A. Salop, R.A. Phaneuf, F.W. Meyer. Phys. Rev. A**16**, 1867 (1977)

[19] P. Hvelplund, A. Andersen. Physica Scripta **26**, 375 (1982)

[20] M.B. Shah, H.B. Gilbody (unpublished)

[21] I. Mancev, Phys. Rev. A **75**, 052716 (2007).

[22] M.L. Vestal, C.R. Blackley, J.H. Futrell, Phys. Rev. A **17**, 1321 (1978)

[23] B. Ziegler, Z. Phys. **136**, 108 (1953)

[24] P. Magadevan, G.D. Magnuson, Phys. Rev**. 171**, 103 (1968)

[25] E.A. Hinds, R. Novick, J. Phys. B **11**, 2201 (1978)

[26] R. Hegerberg, T. Stefansson, M.T. Elford, J. Phys. B **15**, 797 (1982)

[27] R.D. DuBois, Phys. Rev. A **39**, 4440 (1989)

[28] L.I. Pivovar, V.M. Tabuev, M.T. Novikov, Sov. Phys.-JETP, **14**, 20 (1962)

[29] J.L. Forest, J.A. Tanis, S.M. Ferguson et al., Phys. Rev. A **52**, 350 (1995)

[30] A. Itoh, F. Fukuzawa, J. Phys. Soc. Jpn. **48,** 943 (1980)

[31] N.V. de Castro Faria, F.L. Freire, A.G. de Pinho, Phys. Rev. A **37**, 280 (1988)

[32] H. Atan, W. Steckelmacher, M.W. Lucas, J. Phys. B **24**, 2559 (1991)

[33] J.B.H. Stedeford, J.B. Hasted, Proc. Roy. Soc. (London), A **277**, 446 (1955)

[34] F.L. Eisele, S.W. Nagy, J. Chem. Phys. **66**, 883 (1977)

[35] C.F. Barnett, P.M. Stier, Phys. Rev. **109**, 385 (1958)

[36] F.J. de Heer, J. Schutten, H. Moustafa, Physica, **32**, 1793 (1966)

[37] H.B. Gilbody, K.F. Dunn, R. Browning, C.J. Latimer, J. Phys. B **4**, 1040 (1971)

[38] P.R. Jones, F.P. Ziemba, H.A. Moses, E. Everhart, Phys. Rev. **113**, 182 (1959)

[39] H. Martinez, C. Cisneros, J. de Urquijo, I. Alvarez, Phys. Rev. A **38**, 5914 (1988)

[40] F. Wolf, Ann. Physik, **30**, 313 (1937)

[41] D.W. Koopman, Phys. Rev. **154**, 79 (1967)

[42] H.B. Gilbody, J.B. Hasted, J.V. Ireland et al., Proc. Phys. Soc. London **274**, 40 (1963)

[43] Y.Y. Hsu, M.W. Gealy, G.W. Kerby III et al., Phys. Rev. A **53**, 303 (1996)

[44] E.A. Solov'ev, Sov. Phys.-JETP **54**, 893 (1981)

[45] E.A. Solov'ev, Sov. Phys. - Uspekhi **32**, 228 (1989)

[46] Dž. Belkič, R. Gayet, A. Salin, Phys. Rep. **56**, 279 (1979)

[47] Dž. Belkič, R. Gayet, A. Salin, Comput. Phys. Commun. **23**, 153 (1981); *ibid*. **32**, 385 (1984)

[48] Dž. Belkič, *Quantum Theory of High-Energy Ion-Atom Collisions* (Taylor & Francis, London, 2007)

[49] V.P. Shevelko, O. Rosmej, H. Tawara, I.Yu. Tolstikhina, J. Phys. B **37**, 201 (2004)

[50] V.P. Shevelko, H. Tawara, O.V. Ivanov, T. Miyoshi, K. Noda, Y. Sato, A.V. Subbotin, I.Yu. Tolstikhina, J. Phys. B **38**, 2675 (2005)

[51] V.P. Shevelko, I.Yu. Tolstikhina, T. Stöhlker, Nucl. Instr. Meth. B **184**, 295 (2001)

Table 1. Nine-order polynomial fitting parameters used in eq. (4) for the recommended total one-electron capture cross sections shown in Figs. 1-3 and 6-9. The accuracy of fitting is estimated to be within 20%. Last column shows the energy range of the recommended data.

Target A	A_0	A_1	A_2	A_3	A_4	A_5	A_6	A_7	A_8	A_9	Energy range, keV/u
H	**-16.382**	**0.4801**	**-0.1012**	**0.8740**	**-0.0342**	**-0.7440**	**0.1485**	**0.1715**	**-0.0777**	**0.0092**	**$0.04\text{-}2\cdot10^{3}$**
He	**-15.114**	**-0.2623**	**-0.0689**	**-0.0057**	**-0.0007**	**-0.0113**	**-0.0033**	**$2.25\cdot10^{-4}$**	**$2.00\cdot10^{-4}$**	**$1.99\cdot10^{-5}$**	**$10^{-5}\text{-}2\cdot10^{3}$**
He*(1s2s)	**-14.331**	**-0.0353**	**-0.1381**	**-0.1607**	**-0.0251**	**0.00793**	**$6.57\cdot10^{-4}$**	**$-2.15\cdot10^{-4}$**	**$1.03\cdot10^{-5}$**	**0**	**$0.001\text{-}2\cdot10^{3}$**
Ne	**-15.161**	**0.2981**	**-0.1684**	**0.17675**	**-0.3828**	**0.1924**	**-0.0485**	**0.00673**	**$-4.9\cdot10^{-4}$**	**$1.44\cdot10^{-5}$**	**$0.02\text{-}10^{4}$**
Ar	**-15.268**	**0.5824**	**-0.1410**	**-0.1826**	**-0.0553**	**0.0217**	**0.00712**	**-0.00181**	**$-3.40\cdot10^{-4}$**	**$7.24\cdot10^{-5}$**	**$0.001\text{-}2\cdot10^{4}$**
Kr	**-15.036**	**0.2201**	**-0.1462**	**0.0900**	**-0.1505**	**0.03057**	**0.00132**	**$-6.90\cdot10^{-4}$**	**$1.52\cdot10^{-5}$**	**$3.15\cdot10^{-6}$**	**$0.01\text{-}2\cdot10^{4}$**
Xe	**-14.751**	**-0.06056**	**0.02248**	**-0.0184**	**-0.0900**	**0.00905**	**0.00784**	**-0.0022**	**$2.01\cdot10^{-4}$**	**$-5.58\cdot10^{-6}$**	**$0.01\text{-}10^{4}$**

Table 2. Nine-order polynomial fitting parameters used in eq. (4) for the recommended state-selective capture cross sections shown in Figs. 4 and 5. The accuracy of fitting is estimated to be within 20%. Last column shows the energy range of the recommended data.

Reaction	A_0	A_1	A_2	A_3	A_4	A_5	A_6	A_7	A_8	A_9	Energy range, keV/u
He^{+}+He(*1s*2s) → $He(1s^2)$+He^{+}(1s)	**-19.874**	**5.0495**	**-2.7663**	**1.13363**	**-0.4542**	**0.06955**	**$1.36\cdot10^{-4}$**	**$-5.13\cdot10^{-4}$**	**$-5.30\cdot10^{-5}$**	**$8.01\cdot10^{-6}$**	**$0.4\text{-}2\cdot10^{3}$**
He^{+}+He(1s*2s*) → He(1s*2s*)+He^{+}(1s)	**-15.155**	**-0.2458**	**-0.1963**	**-0.2657**	**-0.0631**	**0.02483**	**0.0033**	**-0.00142**	**$1.022\cdot10^{-4}$**	**0**	**0.01-500**

Table 3. Nine-order polynomial fitting parameters used in eq. (4) for the recommended one-electron ionization cross sections shown in Figs. 10 - 16. The accuracy of fitting is estimated to be within 20%. Last column shows the energy range of the recommended data.

Target A	A_0	A_1	A_2	A_3	A_4	A_5	A_6	A_7	A_8	A_9	Energy range, keV/u
H	**-19.067**	**3.214**	**-0.985**	**0.6991**	**-0.4723**	**0.0612**	**0.02669**	**-0.0068**	$\mathbf{1.07\cdot10^{-4}}$	$\mathbf{5.110\cdot10^{-5}}$	$\mathbf{0.3 - 2\cdot10^{4}}$
He	**-19.742**	**3.693**	**-1.126**	**0.5985**	**-0.4442**	**0.1078**	**0.00821**	**-0.0075**	**0.00113**	$\mathbf{-5.552\cdot10^{-5}}$	$\mathbf{0.1 - 10^{6}}$
He*(1s2s)	**-17.104**	**1.798**	**-0.866**	**0.3390**	**-0.0879**	**-0.0114**	**0.00538**	**0.00161**	$\mathbf{-6.94\cdot10^{-4}}$	$\mathbf{6.206\cdot10^{-5}}$	$\mathbf{0.2 - 2\cdot10^{4}}$
Ne	**-18.544**	**3.712**	**-2.078**	**0.7643**	**-0.1786**	**0.02204**	**-0.01174**	**0.00609**	**-0.0012**	$\mathbf{8.081\cdot10^{-5}}$	$\mathbf{0.3 - 10^{5}}$
Ar	**-18.094**	**3.652**	**-1.675**	**0.2253**	**0.05484**	**0.01531**	**-0.03622**	**0.01394**	**-0.0022**	$\mathbf{1.266\cdot10^{-4}}$	$\mathbf{0.2 - 10^{5}}$
Kr	**-17.724**	**3.071**	**-1.554**	**0.5347**	**-0.1441**	**0.03465**	**-0.02475**	**0.01214**	**-0.0025**	$\mathbf{1.892\cdot10^{-4}}$	$\mathbf{0.2 - 3\cdot10^{4}}$
Xe	**-17.743**	**3.192**	**-1.612**	**0.5244**	**-0.2023**	**0.1070**	**-0.04756**	**0.0124**	**-0.0017**	$\mathbf{8.813\cdot10^{-5}}$	$\mathbf{0.2 - 10^{5}}$